Phase Separation of Liquid-Liquid Two-Phase Flow at a T-Junction

L. Yang, B. J. Azzopardi, and A. Belghazi
Multiphase Flow Research Group, Nottingham Fuel and Energy Centre, School of Chemical, Environmental and Mining Engineering, University of Nottingham, University Park, Nottingham NG7 2RD, U.K.

S. Nakanishi
Department of Mechanical and System Engineering, Ryukoku University, Otsu, Japan

DOI 10.1002/aic.10589
Published online September 14, 2005 in Wiley InterScience (www.interscience.wiley.com).

The phase separation of liquid-liquid two-phase flow at a T-junction has been studied using kerosene and deionized water as working fluids and a T-junction with a horizontal main pipe and a vertically upward side arm. Separation data are evaluated by a new criterion: separation efficiency. The results show that the T-junction is highly efficient at separating two immiscible liquids when the flows approaching the T-junction are stratified and when the fractional mass take offs close to the inlet kerosene mass fraction. A new model has been proposed for the phase separation. Comparison between the model and the experimental data shows that the data is well represented by the model. © 2005 American Institute of Chemical Engineers *AIChE J,* 52: 141–149, 2006
Keywords: liquid-liquid flow, T-junction, separation efficiency, ideal separation, model

Introduction

Multiphase flows, the simultaneous flows of more than one phase, are found in a wide range of industrial applications in the chemical and petroleum industries. For example, gas-liquid two-phase flows occur in distillation, absorption, and evaporation; liquid-liquid two-phase flows in extraction; and various two-phase and three-phase flows in heterogeneous chemical reactions in the petrochemical industry. Among these multiphase flows, there is particular interest in the flows in the oil production industry, where crude oil, mixed with natural gas, water, and (occasionally) sand, emerges from wells. Each of these needs to be separated out for economic and safety reasons, especially for offshore wells, before being transported to their destination. Traditionally, large vessels are used for the separation. The separator and necessary support steelwork on offshore platforms are costly. In addition, there is an enhanced risk because of the large inventory of flammable material held in the vessel.

Phase maldistribution almost inevitably occurs when two-phase mixtures are divided at T-junctions. Studies of the phase maldistribution have been reported for gas-liquid, gas-solid, and liquid-solid flows. There is a substantial literature for gas-liquid two-phase flows, with considerable understanding of the important parameters influencing the phase maldistribution for some geometries and flow patterns. Significant quantities of experimental data for gas-liquid flow have been collected, and considerable efforts in flow modeling have been made. Extensive reviews have been published by Azzopardi[1] and Müller and Reimann[2]. Though this topic was initially studied because of the detrimental effect of the maldistribution on downstream equipment, the emphasis has changed more recently to the use of such a junction as a compact partial phase separator. Indeed, such a separator for vapor-liquid flow has been designed and installed successfully on a chemical plant in the U.K. by Azzopardi et al.[3]

In the division of single-phase flow at a T-junction, it has been reported that, to a reasonable approximation, the fluid taken off through the side-arm comes from the segment of main

Correspondence concerning this article should be addressed to B. J. Azzopardi at barry.azzopardi@nottingham.ac.uk..
Current address of L. Yang: Department of Chemical Engineering, Jiangsu Polytechnic University, Changzhou, Jiangsu, China 213016.

pipe nearest the side-arm.[4,5] The position of the chord delimiting the segment moved further away from the side-arm as the fractional take off increased. In their modeling of vertical annular gas-liquid flow, Azzopardi and Whalley[6] suggested that the gas and film were taken off from the segment of main pipe nearest the side-arm. Shoham et al.[7] disagreed with this purely geometrical model. In their approach they followed the ideas of Oranje[8] and Hong,[9] who suggested that as the flow curved into the side-arm, centrifugal forces could push either the gas or liquid to the outside of the limiting arc and, therefore, they would not emerge through the side-arm. They also proposed a damping factor based on viscosity. Versions of the model were developed for annular and stratified flows. Though their model gives reasonable prediction of some data, there is evidence that it might not cover all the relevant mechanisms. Rea and Azzopardi[10] suggested that falling of liquid from the main pipe into the side-arm, as in a dam break, was relevant.

There are far fewer publications on other phase combinations, with none reported for liquid-liquid flows. This article rectifies the lack of data for liquid-liquid flows. Kerosene and deionized water were used as working fluids. A T-junction with a horizontal main pipe and a vertically upward side-arm was employed. The effect of the flow rates of the two phases was examined. A new criterion, separation efficiency, was proposed to optimize operational conditions for phase separation at the T-junction. Because of the poor performance of models originating from work on gas-liquid flows, a new model based on observations of the behavior of the interface and the geometrical model proposed by Azzopardi and Whalley[6] was developed to fit the present data.

Separation Efficiency

A new criterion

In order to assess the phase separation results and optimize the operation conditions for the phase separation at junctions, a new criterion, separation efficiency, has been proposed. Before discussing two-phase flow at a T-junction, it is useful to define some parameters. Referring to Figure 1, $\dot{m}$ and x represent, respectively, the mass flowrate and kerosene mass quality (ratio of kerosene mass flowrate to total mass flowrate); and subscripts K and W refer to kerosene and water, respectively. The inlet pipe is given the subscript 1, the straight arm (the run) 2, and the side-arm (the branch) 3. Another parameter often used for two immiscible liquids is water cut, which is defined as water volume fraction within the flow.

Traditionally, the results of phase separation at a T-junction are presented by using the fraction of one phase taken off versus that of another, as shown in Figure 2. The fractions of kerosene and water taken off can be written as F_K and F_W, respectively, as follows

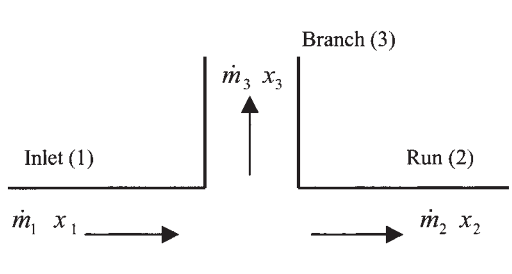

Figure 1. Parameters of two-phase flow at a T-junction.

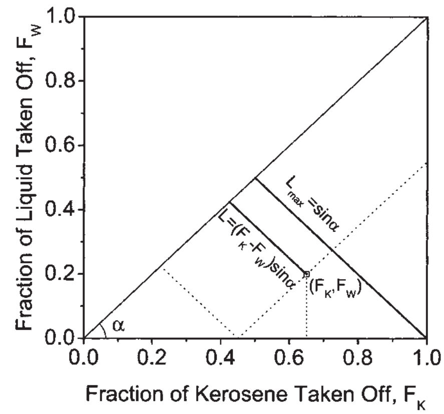

Figure 2. A new criterion, separation efficiency, derived from the traditional expression for separation results of a T-junction.

$$F_K = \frac{\dot{m}_{K3}}{\dot{m}_{K1}} \tag{1}$$

$$F_W = \frac{\dot{m}_{W3}}{\dot{m}_{W1}} \tag{2}$$

In Figure 2 the abscissa is the fraction of kerosene taken off F_K, and the ordinate is the fraction of water taken off F_W. A diagonal line between (0,0) and (1,1) represents equal split, i.e., no separation occurs if data points lie on this line. This line divides the figure area into two parts; data in the lower part correspond to kerosene flowing preferentially into the side-arm and vice versa. The further from the equal split line, the better the separation. The corners of this figure, (0,1) or (1,0), are conditions of complete separation. The closer the data to the corners, the better the separation. The distance, L, from the equal split line to a datum point, a good measure of the separation effected, is

$$L = (F_K - F_W)\sin\alpha \tag{3}$$

where α is the angle between the diagonal line and the abscissa. The separation efficiency η is now defined as the ratio of the actual separation to the complete separation, $L_{max} = sin\alpha$, i.e.,

$$\eta = \frac{L}{L_{\max}} = |F_K - F_W| \tag{4}$$

where the absolute value is used because experimental data may be plotted on either side of the equal split line, depending on which phase dominates the take off. Eq. 4 indicates that the separation efficiency is the difference of the fractions of take off between the two phases. In other words, data points lying on a straight line parallel to the diagonal line have the same separation efficiencies. It can be seen that they may have different mass qualities in two outlets while they have the same

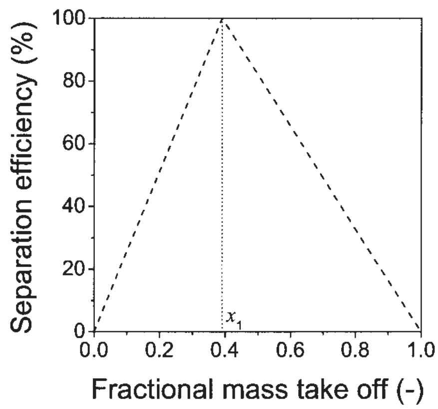

Figure 3. Method of presentation of separation efficiency and ideal separation.

separation efficiencies. Usually, the separation efficiency is <100%.

Ideal separation

If two phases take off in the side-arm separately in order, an ideal phase separation occurs. This section considers the ideal phase separation. This confines the possible separation efficiency and provides pointers as to the efficient operation of T-junction phase separators. Kerosene dominates the take off if data lie in the diagonally lower part of Figure 2, with water dominating when the data are in the diagonally upper part. For the former, there are two ideal separation data lines. The first ideal separation data line, as the fractional mass taken off increases, is the abscissa in Figure 2, and the second line is the vertical line opposite the ordinate. Between them, a bottom right corner represents complete separation. For the point located exactly on the corner, pure kerosene and pure water are separated from the inlet mixture, respectively, to the side-arm and to the run. It means that the mass quality in the side-arm x_3 is equal to 1, and the quality in the run x_2 is 0. Meanwhile, the separation efficiency reaches an ideal peak of 100%. When this ideal efficiency peak occurs, the fractional mass take off can be written as:

$$\frac{\dot{m}_3}{\dot{m}_1} = x_1 \tag{5}$$

For the first ideal separation line, pure kerosene emerges from the side-arm and the mixture flows out from the run. It means that the fraction of water taken off F_W is 0, and the mass quality x_3 is equal to 1. An equation can be derived for this line, that is:

$$\eta = F_K = \frac{1}{x_1}\frac{\dot{m}_3}{\dot{m}_1} \quad \left(\frac{\dot{m}_3}{\dot{m}_1} \leq x_1\right) \tag{6}$$

Data lying on this line are associated with pure kerosene emerging through the side-arm. Whereas, for the second ideal line, pure water flows out from the run and the mixture emerges from the side-arm. The quality in the run x_2 is equal to 0. Similarly, an equation for this ideal line can be derived as:

$$\eta = 1 - F_W = -\frac{1}{(1 - x_1)}\frac{\dot{m}_3}{\dot{m}_1} + \frac{1}{1 - x_1} \quad \left(\frac{\dot{m}_3}{\dot{m}_1} \geq x_1\right) \tag{7}$$

This represents cases where pure water emerging through the run is sought. To identify optimal take off conditions, split data are plotted as separation efficiency η versus fraction of mass taken off $\dot{m}_3/\dot{m}_1$, and as shown in Figure 3 where Eq. 6 is represented by the upwardly inclined line and Eq. 7 by the downwardly inclined line. The interception point represents complete separation. For the kerosene dominated take off, the

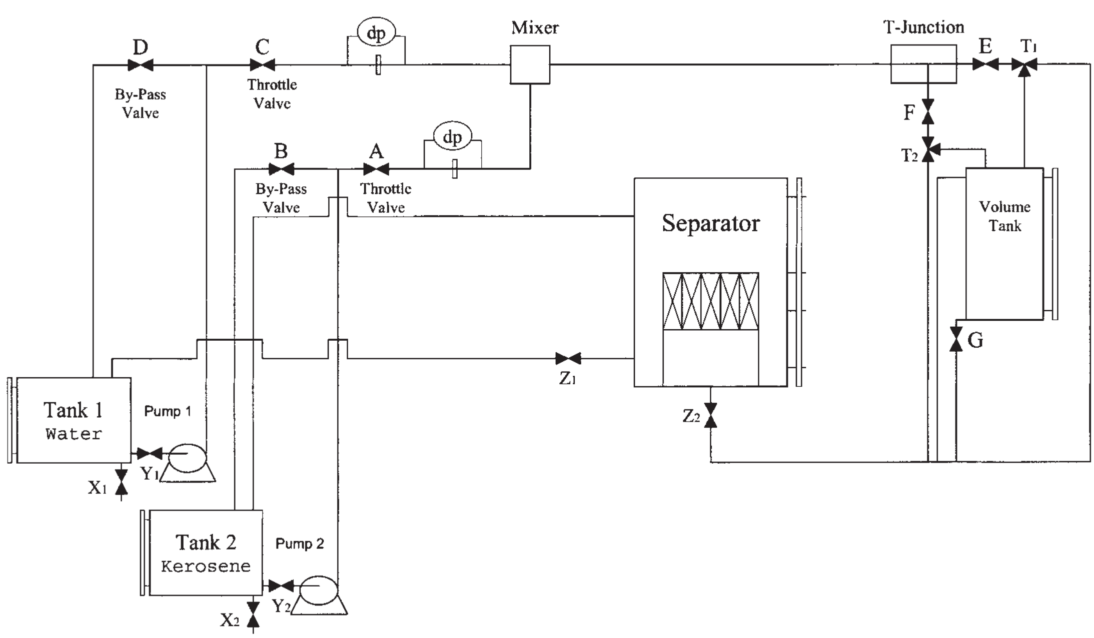

Figure 4. Experimental system.

Table 1. Physical Properties of Liquids

	Kerosene	Deionized Water
Density (kg/m^3)	796	998
Viscosity (kg/ms)	0.0021	0.001
Interfacial tension (N/m)	0.024	

complete separation occurs when the fractional mass take off is equal to the inlet mass quality, x_1. A similar analysis can be developed for water dominated take off, with complete separation occurring at the water inlet quality, i.e. $(1 - x_1)$.

Experimental

The experiments reported below were carried out on a facility in the laboratories of the School of Chemical, Environmental and Mining Engineering, University of Nottingham. Previously it was used for measurements of drop sizes in liquid-liquid flows[11] and of the effect of bends[12] on such flows. It is shown schematically in Figure 4. Water and kerosene are pumped from their respective storage tanks, metered, and introduced into a mixer. The flow rates of kerosene and water into the main pipe were metered by calibrated orifice plates connected to differential pressure cells. In the mixer the water is introduced axially, while the kerosene was introduced into the test section through a large number of holes in the pipe wall, which were angled downstream at 15^o to the axis. The mixture flows along a 3.1 m long horizontal pipe to the T-junction. The run is 2.0 m long. The vertically upward side-arm was 1.2 m tall before connecting to another horizontal pipe section. All pipes are of 0.0674 m internal diameter. There are valves to control the split of the flow at the ends of both outlets. Beyond these, the flow enters a large phase separator, i.e., a vertically cylindrical vessel 2.4 m tall by 2.5 m in diameter containing 34 coalescer cartridges each 0.15 m diameter and 1 m long. The flow from each of the two outlets could be diverted in turn into a separate tank for a fixed time where the phases were allowed to separate under gravity and the volumes measured. This gave phase flow rates. The liquids used in experiments were kerosene and deionized water. Their properties are listed in Table 1.

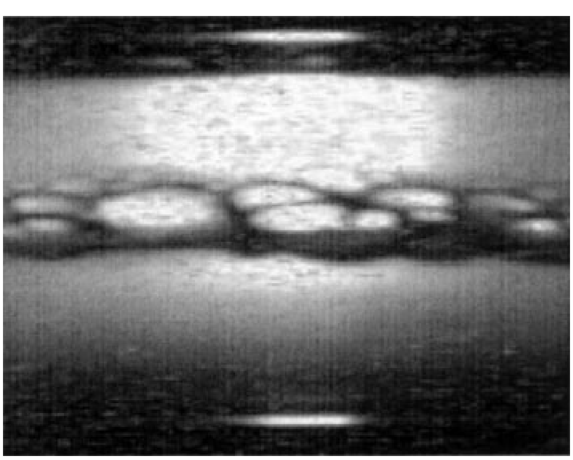

Figure 5. Stratified flow with mixing at the interface.

Three layers: oil layer at the pipe top and water layer at the pipe bottom; between them, a mixed layer with oil drops.

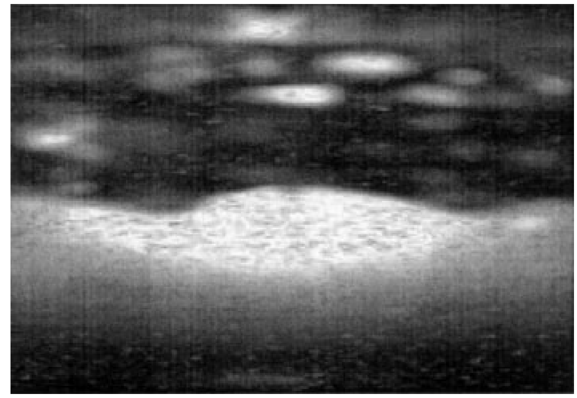

Figure 6. Mixed layer expands almost up to the top of the pipe when the mixture velocity increases.

Results

Flow patterns and their occurrence

The flow pattern during the present experiments was studied by observing the flow through the transparent pipe wall with both the naked eye and by using a high speed video camera. The observation is made 2.8m downstream of the mixer, as shown in Figure 4. In order to diminish deformation of the pictures caused by refraction at the cylindrical pipe wall, the recording was performed with a square sided, $0.2 \times 0.2 \times 0.2$ m, acrylic resin box filled with water mounted around the pipe. Backlighting produced the best pictures.

When two immiscible liquid phases flow concurrently in a pipe, a number of flow patterns are observed. If the mixture velocity is very low, there are only two layers present, i.e., oil flowing over water. As the water velocity is increased, transition to other regimes occurs. In the present study, at a water velocity of 0.1 m/s and kerosene velocity of 0.06 m/s, the flow pattern was stratified flow (ST). Increasing water velocity to 0.15 m/s led to the formation of large oil drops at the interface between the water layer and oil layer, especially at the area close to the pipe wall; see, for example, the 10 mm $\times$ 20 mm oval drop shown in Figure 5. This may be because the region near the wall has relatively higher shear stress due to steep velocity gradients and kerosene at the interface in this region is easily broken into drops under this shear stress. Further increasing the water velocity caused these oil drops to break up into smaller spherical drops.

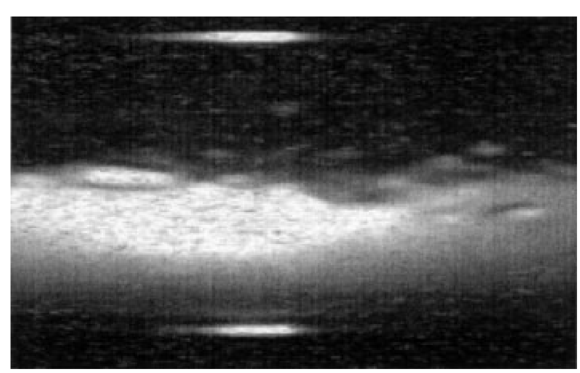

Figure 7. Small droplets burst into the water layer as mixture velocity increases further.

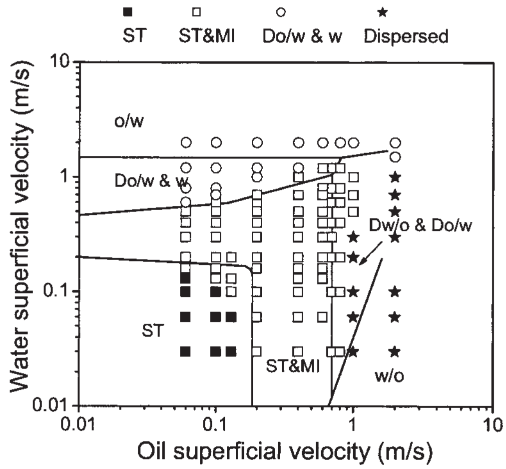

Figure 8. Flow patterns plotted on the flow pattern map of Trallero et al.[13]

Pipe diameter = 0.0674m, horizontal orientation.

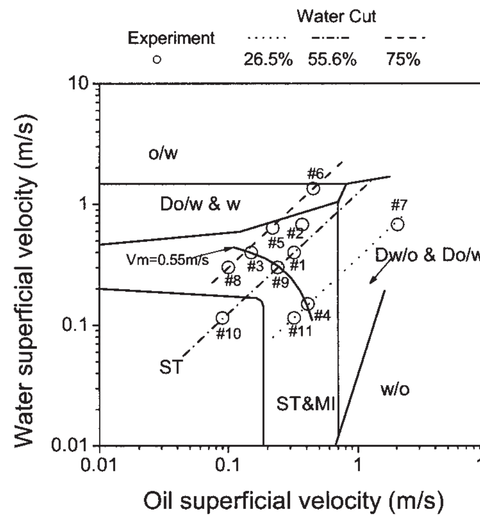

Figure 9. Inlet flow conditions plotted on the flow pattern map of Trallero et al.[13]

These are distributed over the whole interface and form a mixed layer. As the water velocity increases, the mixed layer expands into the oil layer and the drops become smaller. This flow pattern is termed stratified flow with mixing at interface (ST&MI). When the water velocity is increased to 0.6 m/s, the mixed layer extends to the top of the pipe, as shown in Figure 6, and the oil drops at the interface between the water layer and the mixed layer enter the water layer, as shown in Figure 7. That makes the water layer become a dilute dispersion of oil in water (o/w) where a few oil drops are distributed with concentration gradient from the interface to the pipe bottom. At these conditions, the water is a continuous phase across the whole sectional area, and a new flow pattern, i.e., dispersion of oil in water above a water layer (Do/w&w), is developed.

If, on the other hand, the oil velocity is increased, the flow pattern also changes. In the present study, at a water velocity of 0.1 m/s and an oil velocity of 0.1 m/s, the flow is ST. Increasing the oil velocity to 0.2 m/s results in the ST&MI pattern. Further increasing the oil velocity to 1.0 m/s leads to the disappearance of a clear kerosene layer, and a new dispersed flow pattern, i.e., dispersion of water in oil and dispersion of oil in water (Dw/o&Do/w), forms. However, at these conditions a thin water film of about 5mm thickness still exists at the pipe bottom.

Figure 8 shows a comparison between the flow pattern map of Trallero et al.[13] and the present data. Trallero et al. employed an acrylic resin pipe of 50 mm internal diameter in contrast to the UPVC pipe of 67.4 mm used here. It can be seen that for the segregated flow patterns, i.e., the ST and ST&MI flow regimes, there is good agreement. The ST&MI data cover a slightly larger area than predicted by Trallero et al. The dispersed flow regimes, the area of the Do/w&w in this study, is larger than that of Trallero et al.

Phase separation

In the present work, phase maldistributions have been measured for kerosene-water flow. Obviously, the behavior of two-phase flow at a T-junction highly depends upon the flow patterns approaching the T-junctions. Therefore, flow conditions at different flow patterns have been selected to check their effects on the phase separation. Table 2 shows these conditions.

The superficial velocities of the kerosene, V_{sk}, and the water, V_{sw}, for these conditions are plotted on the flow pattern map of Trallero et al.[13], Figure 9. Five flow patterns were encountered, i.e., ST, ST&MI, Do/w&w, Dw/o&Do/w, and o/w regimes. The inlet conditions in Table 2 are at water cuts of 75%, 55.6%, and 26.5%. The split data is tabulated by Yang.[14]

Generally, phase separation results for kerosene-water two-phase flow at this T-junction are promising. Figure 10 shows typical results. Almost all data lie on the water fraction = 0 and kerosene fraction = 1 lines, Figure 10a. These results indicate

Table 2. Inlet Conditions for Phase Separation at the T-Junction

Run No.	Side-Arm Orientation	Mixture Velocity (m/s)	Water Cut W_c (%)	V_{sw} (m/s)	V_{sk} (m/s)	Inlet Quality, x_1
#1	Vertical up	0.72	55.6	0.40	0.32	0.39
#2		1.05	65	0.68	0.37	0.30
#3		0.55	75	0.40	0.15	0.23
#4		0.56	26.5	0.15	0.41	0.69
#5		0.86	75	0.64	0.22	0.22
#6		1.80	75	1.35	0.45	0.21
#7		2.71	26.5	0.68	2.03	0.69
#8		0.40	75	0.30	0.10	0.21
#9		0.54	55.6	0.30	0.24	0.39
#10		0.20	55.6	0.115	0.09	0.39
#11		0.43	26.5	0.115	0.32	0.69

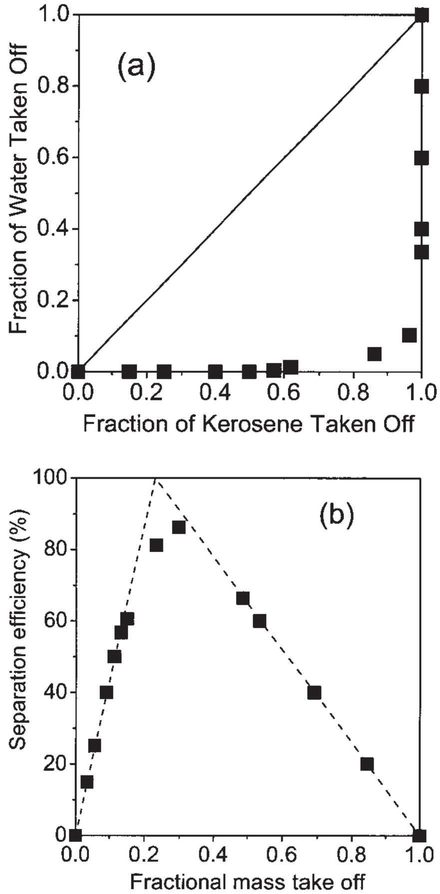

Figure 10. Typical phase separation results. Flow conditions: #3 at mixture velocity = 0.55 m/s and water cut = 75%.

(a) Traditional presentation of separation results, (b) Separation efficiency.

ideal separation, and the separation efficiencies are mostly along the ideal separation lines, Figure 10b, except at the area near the ideal separation peak (fractional mass take off = the inlet mass quality x_1). The separation efficiency peak can reach values of greater than 80%. The highest separation efficiencies in this case are 57% at a fractional mass take off of 0.13 for just kerosene emerging and 67% at the fractional mass take off 0.48 for just water emerging from the run.

When the inlet flow is ST&MI and the mixture velocity is constant, Figure 11 shows that the water cut has a significant effect on separation. The higher the water cut, the higher the peak separation efficiency achieved. For example, the peak efficiency reaches 86% for water cut = 75%, 82% for 55.6%, and only 62% for 26.5%. The separation efficiency peak for every water cut can be achieved when the fractional mass take off is set to near the inlet quality. There is an obvious effect of mixture velocities at a water cut of 55.6%. The peak efficiency, 94%, is achieved for run #10 with the lowest mixture velocity in the ST regime when the fractional mass take off is equal to the inlet mass quality x_1. The higher the mixture velocity, the lower the separation efficiency peak achieved. Again, at both the lower side and the higher side of the fractional mass take off, the experimental data points are located on the ideal separation lines. This means the single pure phase can also be separated from the inlet mixture either through the side-arm or through the run.

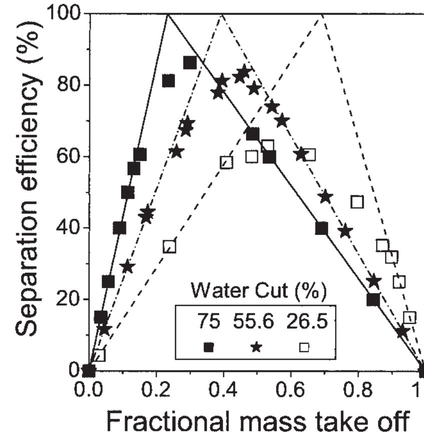

Figure 11. Effect of water cut on the phase separation. Mixture velocity = 0.55 m/s.

At a higher water cut (75%), Figure 12, the mixture velocities also significantly affect the separation results. As for 55.6%, a higher mixture velocity results in a lower peak sep-

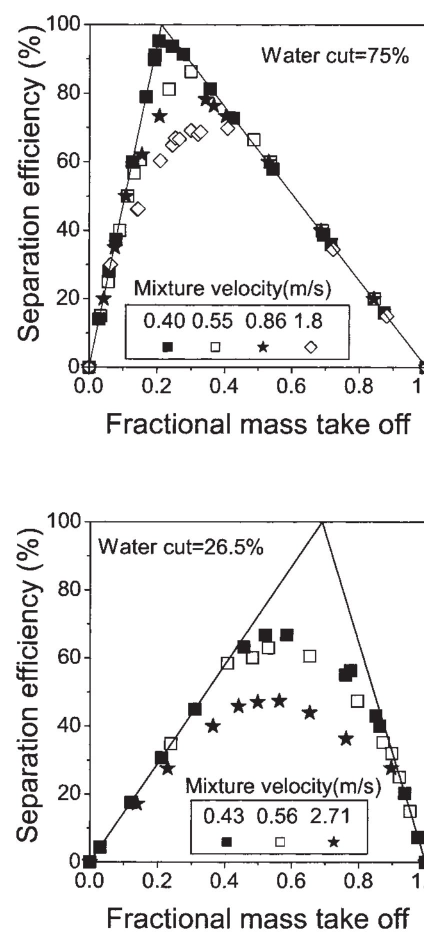

Figure 12. Effects of the mixture velocity on the phase separation: (a) Water cut = 75%, (b) Water cut = 26.5%.

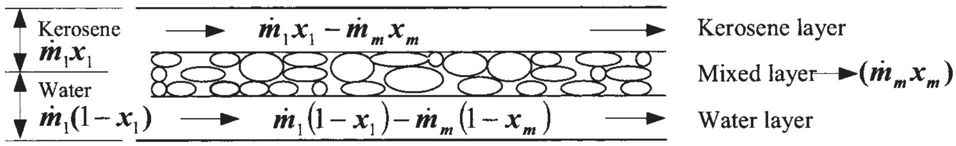

Figure 13. Idealized ST&MI flow pattern for two-phase flow in a pipe.

aration efficiency. The separation efficiency peak for run #8 at a mixture velocity 0.4m/s, which is within the ST&MI regime, can reach 97%; for run #6 (mixture velocity = 1.80m/s, dispersed flow), the peak value drops to 69%. Similarly, at the lower water cut studied, the separation efficiency peak decreases as the mixture velocity increases, and all the separation efficiency peaks are less than 67%. At run #7 with mixture velocity 2.71m/s, which is in the Dw/o&Do/w regime, the separation efficiency peak drops down to 50%.

Discussion

Model of separation

The parameters for the flow at the T-junction are defined as shown in Figure 1. Based on the observation of flow pattern for the ST&MI, there are three layers in the liquid-liquid flow, as shown in Figure 5. Although the interfacial layer is wavy, it is assumed that the interfacial layer is separated by two fixed flat planes, which are idealized as shown in Figure 13. Azzopardi

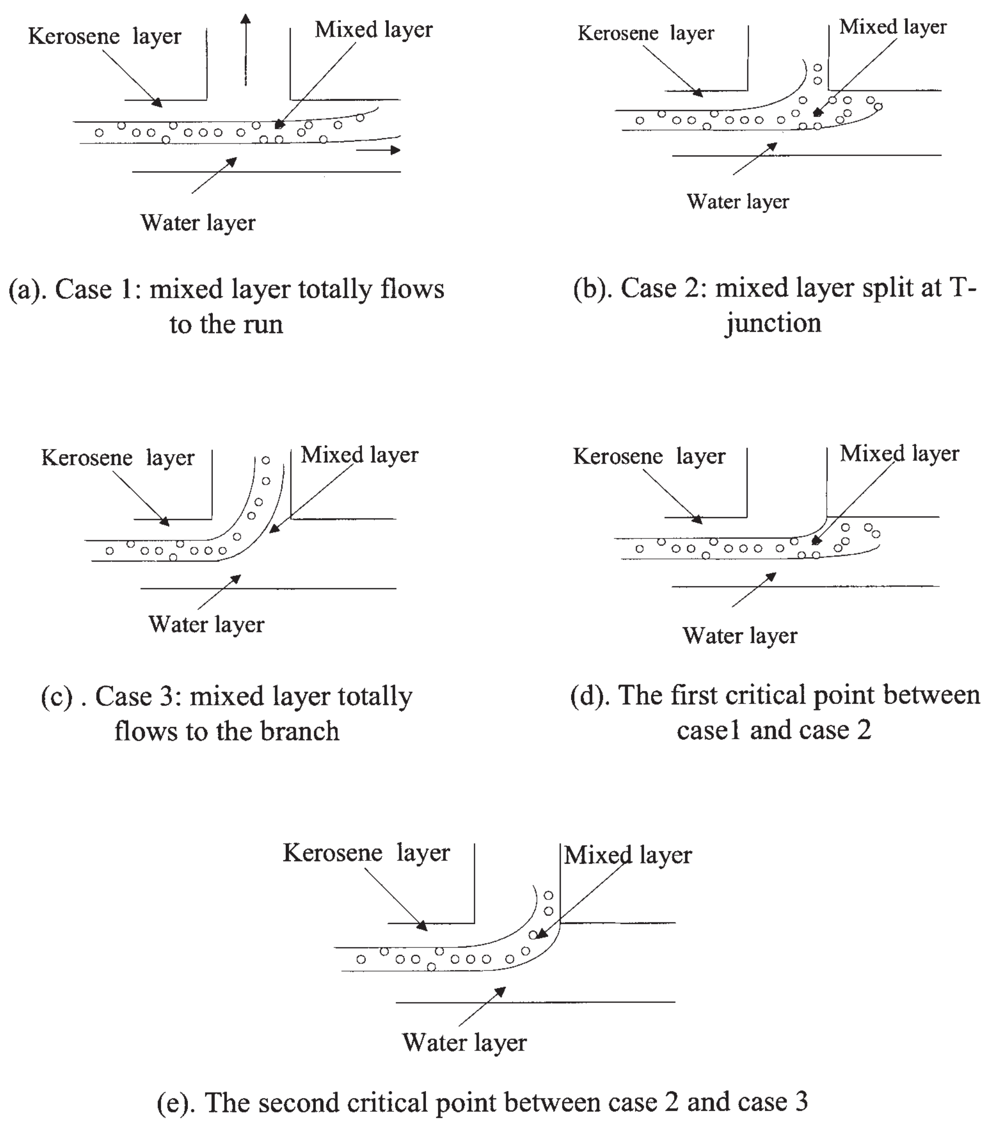

Figure 14. Three cases and two transition points of the elementary model for a T-junction with a vertical upward side-arm.

Table 3. Characteristics of the Elementary Model for the Upwards Side-Arm Case

Case	Fluid Taken Off	$\dot{m}_3$ or $\dfrac{\dot{m}_3}{\dot{m}_1}$	x_3 or x_2
Case 1	Kerosene only Kerosene clear cut	$\dot{m}_3 \leq \dot{m}_1 x_1 - \dot{m}_m x_m$	$x_3 = 1$
First transition point	Same as Case 1	$\dfrac{\dot{m}_3}{\dot{m}_1} = x_1 - \dfrac{\dot{m}_m}{\dot{m}_1} x_m = \left(\dfrac{\dot{m}_3}{\dot{m}_1}\right)_{c1}$	$x_3 = 1$
Case 2	Kerosene and water	$\dot{m}_3 \geq \dot{m}_1 x_1 - \dot{m}_m x_m$ and $\dot{m}_3 \leq \dot{m}_1 x_1 + \dot{m}_m (1 - x_m)$	$x_3 = x_m + (1 - x_m)\left(\dfrac{\dot{m}_3}{\dot{m}_1}\right)_{c1}\left(\dfrac{\dot{m}_1}{\dot{m}_3}\right)$
Second transition point	Same as Case 2 Water clear cut in the run	$\dfrac{\dot{m}_3}{\dot{m}_1} = \left(\dfrac{\dot{m}_3}{\dot{m}_1}\right)_{c1} + \dfrac{\dot{m}_m}{\dot{m}_1} = \left(\dfrac{\dot{m}_3}{\dot{m}_1}\right)_{c2}$	$x_3 = \dfrac{x_1}{x_1 + \dfrac{\dot{m}_m}{\dot{m}_1}(1 - x_m)}$ or $x_2 = 0$
Case 3	Kerosene and water Water clear cut in the run	$\dot{m}_3 \geq \dot{m}_1 x_1 + \dot{m}_m (1 - x_m)$	$x_3 = \dfrac{\dot{m}_1}{\dot{m}_3} x_1$ or $x_2 = 0$

and Whalley[6] developed a geometrical model for the phase maldistribution at a T-junction. In their modeling of vertical annular gas-liquid flow, they suggested that the gas and liquid taken off were the gas and liquid film from the segment of the main pipe nearest the side-arm. According to this geometrical model, the ST&MI flow approaching the T-junction in the present study can appear consequently as following three cases as the take off increases: (1) The mixed layer flows under the side-arm and goes to the run completely, as shown in Figure 14a. (2) The mixed layer is divided by the downstream T-junction corner, as shown in Figure 14b. (3) The mixed layer flows over completely to the side-arm, as shown in Figure 14c.

There are two transition points, respectively, between Cases 1 and 2, and between Cases 2 and 3. The first transition point between Cases 1 and 2, as shown in Figure 14d, indicates that the fluid taken off in the side-arm is pure kerosene (kerosene clear cut) until the take off increases beyond this transition value and case 2 is developed. The second transition point between Cases 2 and 3, as shown in Figure 14e, indicates that the fluid in the run is pure water (water clear cut) after the take off increases beyond this transition value. The model equations of the mass flowrates and qualities for these three cases and two transition points have been derived theoretically by using mass balance, as shown in Table 3. Figure 15 shows the model characteristics. It can be seen from the characteristics of the elementary model that this model depends only upon two parameters, i.e., mass flow rate $\dot{m}_m$ and quality x_m in the mixed layer, assuming the inlet mass flow rate $\dot{m}_1$ and quality x_1 are given. These two parameters have not been measured experimentally in this study but derived indirectly by correlating the experimental data with the model equations in Table 3.

The effect of the water cut on the parameters of the model is shown in Figure 16. As the water cut increases, the kerosene layer at the pipe top becomes thinner; therefore, the first transition point moves to the lower side of the fractional mass take off. It is interesting that all the quality in the mixed layer x_m for these three runs in the Figure is approximately equal to 0.65. It is equivalent to a water cut of 30% in this layer. It should also be noticed that lower water cut enlarges the span of Case 2. The effect of the mixture velocity is strongest at low take off. As the mixture velocity increases, the first transition point appears at lower fractional mass take off and the span of the mixed layer taken off also increases. The reason is probably because the thickness of the mixed layer increases and the thickness of single-phase layers decreases as the mixture velocity increases at the same water cut.

It is noted that to complete the new model, empirical relationships developed from experimental data have been employed to produce closure. However, the proposed method does provide a framework that, with a fuller description of the three layers approaching the junction, could provide a predictive method.

Conclusions

In this study, a new criterion, separation efficiency, has been proposed for the assessment of the phase separation of two-phase flows at T-junctions. From this criterion, an ideal separation model, which limits the highest possible separation efficiency with varying the fractional mass take off, has been built up. This model also gives a clue as to how to operate the T-junction system efficiently.

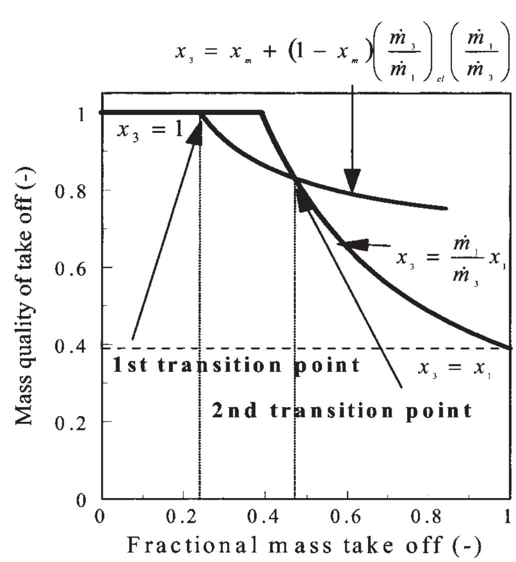

Figure 15. Characteristics of the elementary model.

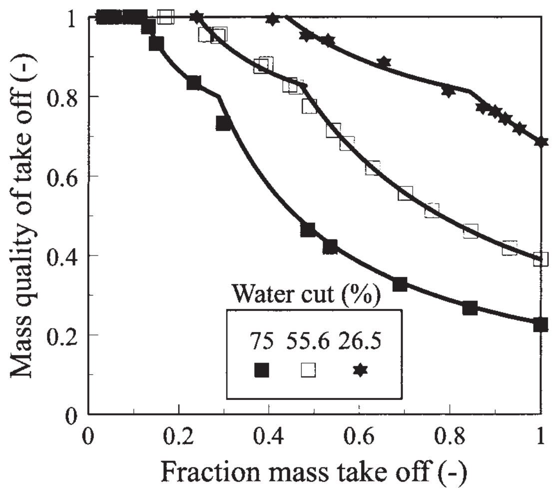

Figure 16. Effect of the water cut on the fit of the elementary model.

Mixture velocity = 0.55 m/s.

A T-junction with a horizontal main pipe and a vertically upward side-arm was employed. Experiments for kerosene-water two-phase flow have been designed to examine the phase separation at various operating conditions.

The T-junction is suitable as a partial phase separator. Higher water cuts are beneficial for phase separation, while higher mixture velocity within the dispersed flow regimes is detrimental. It is found that the phase separation is highly effective when the inlet flows approaching the T-junction are within the segregated flow regimes and the fractional mass take off is set to near inlet mass quality.

The elementary model proposed in the present study correctly predicts all the characteristics of the experimental data. However, it requires information of the incoming flow, which is currently provided from the experiments.

Notation

α = angle between equal split line and abcissa
F = fraction taken off through side-arm
L = distance from the equal split line to the datum
$\dot{m}$ = mass flow rate, kg/s
x = mass fraction of kerosene

Greek letters

η = separation efficiency

Subscripts

K = kerosene
max = maximum
W = water
1 = inlet pipe
2 = run pipe
3 = side-arm

Literature Cited

1. Azzopardi BJ. Phase separation at T-junctions. *Multiphase Sci Technol.* 1999;11:223-329.
2. Müller U, Reimann J. Redistribution of two-phase flow in branching conduits: A Survey. Proc. Int. Conf. Multiphase Flows, Tsukuba, Japan, September 24-27, 1991;85-107.
3. Azzopardi BJ, Colman DA, Nicholson D. Plant application of a T-junction as a partial phase separator. *Chem Eng Res Design.* 2002; 80:87-96.
4. McNown JS. Mechanics of manifold flow. *Trans Amer Soc Civil Eng.* 1954;119:1103-1142.
5. Charron Y, Whalley PB. Gas-liquid annular flow at a vertical tee junction, Part I. Flow separation. *Int J Multiphase Flow.* 1995;21:569-589.
6. Azzopardi BJ, Whalley PB. The effect of flow pattern on two phase flow in a T junction. *Int J Multiphase Flow.* 1982;8:491-507.
7. Shoham O, Brill JP, Taitel Y. Two-phase flow splitting in a tee junction—Experiment and modelling. *Chem Eng Sci.* 1987;42:2667-2676.
8. Oranje L. Condensate behavior in gas pipelines is predictable. *Oil Gas J.* 1973;39-44.
9. Hong KD. Two-phase flow splitting at a pipe tee. *J Petroleum Tech.* 1978;290-296.
10. Rea S, Azzopardi BJ. The split of horizontal stratified flow at a large diameter T-junction. *Chem Eng Res Design.* 2001;79:470-476.
11. Simmons MJH, Azzopardi BJ. Drop size distributions in dispersed liquid-liquid pipe flow. *Int J Multiphase Flow.* 2001;27:843-858.
12. James PW, Azzopardi BJ, Graham DI, Sudlow CA. The effect of a bend on droplet size distribution in two-phase flow. Proc. 7th Int. Conf. on Multiphase Flow in Industrial Plants, Bolonga, Italy, September 19-23, 2000;211-222.
13. Trallero JL, Sarica C, Brill JP. A study of oil-water flow patterns in horizontal pipes. *SPE Production and Facilities.* 1997;165-172.
14. Yang L. Liquid-liquid two-phase flows at T-junctions and through expansions. PhD Thesis. University of Nottingham, 2003.

Manuscript received May 28, 2004, and revision received April 29, 2005.